The Effect of Resolution on Terrain Feature Extraction

S. T. Arundel
U.S. Geological Survey
Center of Excellence for Geospatial Information Science
Rolla, MO
sarundel@usgs.gov

Wenwen Li, Xiran Zhou
School of Geographical Sciences & Urban Planning
Arizona State University
Tempe, AZ
{wenwen, xrzhou}@asu.edu

Abstract—**Recent increase in the production of high-resolution digital elevation models (DEMs) from lidar data has led to interest in their use for terrain mapping. Although the impact of different resolutions has been studied relative to terrain characteristics like roughness, slope and curvature, its relationship to the extraction of terrain features remains unclear. To address this question, this study tests the impact of four resolutions on the capture of glacial cirques from DEMs. Mean curvature was derived from one arc-second, one-third arc-second, one-ninth arc-second and half meter DEMs representing a cirque-covered mountainous region southwest of Lake Tahoe, California. Using a GEOBIA workflow, ridge objects were identified, and three scales - via the multi-resolution scale parameter (SP) - of objects bordering the ridges were classified as cirque objects. The resulting classifications were compared to reference cirques digitized at a scale of ~1:10,000. Results show that the one-third arc-second DEM produces the set of cirque objects most closely resembling the reference cirques. The one-ninth arc-second DEM afforded the second-best classification. These results emphasize the importance in carefully choosing resolution relative to the features extracted, rather than using the highest resolution data available. In the case of GEOBIA workflows, the choice of scale parameter is equally important.**

I. INTRODUCTION

The growing accessibility of digital elevation models at increasingly higher resolution, and continued improvements in computer computation and modelling software are encouraging unprecedented opportunities for geomorphologists to make advances in landform mapping [1]. Automatic classification of surface shapes fosters more objective portrayal of forms and, particularly, their boundaries. While accuracy may also be increased, the introduction of error by automation must be minimized through the proper choice of classification (and partitioning) algorithms, study area size, collection scales and DEM resolutions (grid cell size).

Most terrain *attributes* derived directly from DEM pixels, like slope and curvature, are known to vary with changing DEM resolutions [2], and many efforts to automate landform classification depend upon the inferred relationship between particular terrain attributes and erosional or depositional processes [3]. However, the approach of classifying these attributes on a cell by cell basis is constraining in various features, including difficulty in capturing topological relationships between landscape objects and referencing the scale of analysis to the raster resolution. Geographic object-based image analysis (GEOBIA), in which the pixel-based dataset is segmented into elementary forms before classification is a suggested approach employed to overcome these limitations [4]. However, the impact of changing DEM resolution on terrain *objects* and their classification should be better understood, as choice of resolution is an important step in processing data.

This paper assesses how object representation of one particular landform type (glacial cirques) changes with four increasingly larger resolutions of DEMs produced from the same lidar dataset. The cirque objects are created using basic semantics and GEOBIA technology, and tested against a reference dataset.

Cirques as landforms offer an ideal test case because of their characteristic topographic signature in mountainous regions [5]. Cirque delineation is fairly straight-forward in areas where they are clearly defined, making them good automated test features, and identifiable as amphitheatre-like depressions in alpine glacial terrain. Because cirque sizes studied across several regions vary from about 15 to 25 acres (~6 to 10 hectares) [6], objects smaller than 10 acres were not analysed in this study.

II. STUDY AREA

The study area is composed of a 10,000 km^2 area in the east-central Sierra Nevada mountain range located just west and southwest of Lake Tahoe (Figure 1). Elevation ranges in the study area from 1798 m above sea level (a.s.l.) to 3043 m a.s.l.

The Sierra Nevada mountain range is the longest and highest in the coterminous United States. The backbone of the range is mostly Mesozoic granite, formed where a chain of volcanoes intruded into the older Palaeozoic rock. By the Late Cretaceous, the deep granite had been uncovered by erosion. The range developed as either the eastern basin subsided, or the exposed

PeerJ Preprints | https://doi.org/10.7287/peerj.preprints.27072v1 | CC0 Open Access | rec: 30 Jul 2018, publ: 30 Jul 2018

granite was uplifted along a north-south fault east of the range [7]. The study area exhibits numerous cirques and other typical glacial features like arêtes, tarns, and glacial moraines as evidence of glacial erosion. As of 2008, over 100 glaciers still existed in the Sierra Nevada mountain range [8].

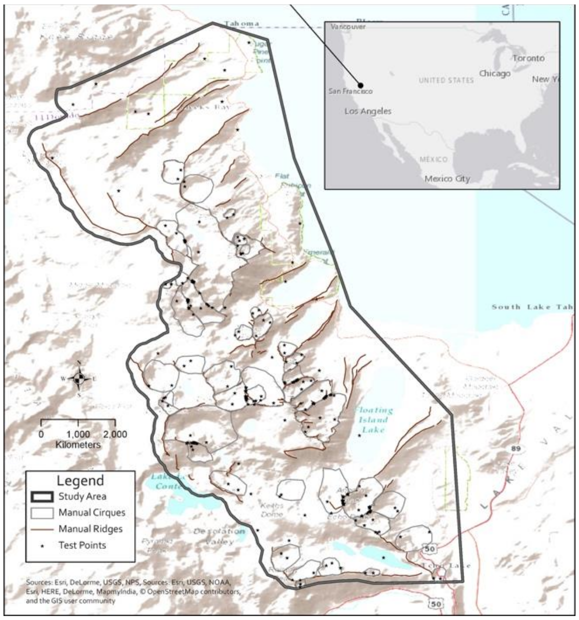

Figure 1. Study area in the east-central Sierra Nevada mountain range, showing hand-drawn ridges, glacial cirques, and stratified random test points.

In August of 2010, lidar data were collected for the Tahoe Basin, with an average native pulse density of > 8 pulses per square meter over terrestrial surfaces. The data delivered from this collection included a point cloud with an average ground point density of 2.26 points per square meter, and a half-meter resolution DEM, which were incorporated into The National Map's one-ninth, one-third, and one arc-second datasets. The new one-meter dataset was not yet in production. The availability of a range of resolutions allows analysis of the impact these resolutions have on feature delineation and classification.

III. Methods

The semantics-based glacial cirque classification workflow is based on that developed for a test region in Austria [9]. The results and detailed methods of a modified workflow tested in the study area are reported by [10].

The same general steps are followed for each of the four DEM resolutions (Figure 2). First, a mean curvature raster is derived from the study area (plus buffer) DEM. Baseline objects are then created in a GEOBIA software using the multiresolution segmentation (MRS) algorithm, setting the scale parameter (SP) to 5 for all resolutions except the 1 arc-second dataset, for which an SP of 1 was required to generate sufficiently small objects for future segmentation and classification. Baseline objects were classified as ridges if mean curvature exceeded a manually selected threshold value.

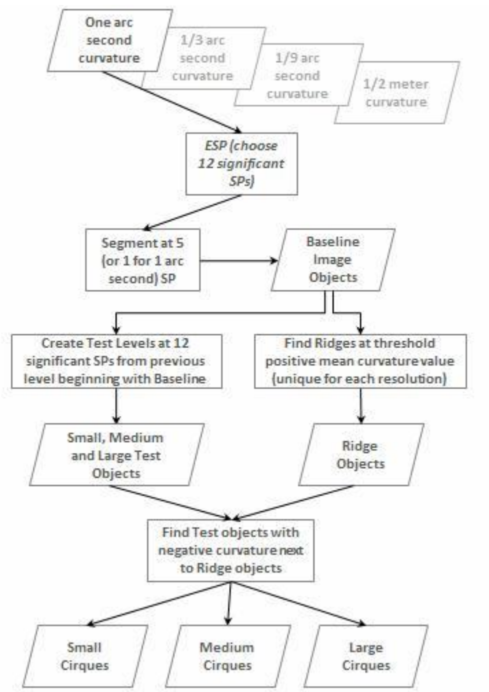

Figure 2. Workflow for producing three cirque sizes from four DEM resolutions.

PeerJ Preprints | https://doi.org/10.7287/peerj.preprints.27072v1 | CC0 Open Access | rec: 30 Jul 2018, publ: 30 Jul 2018

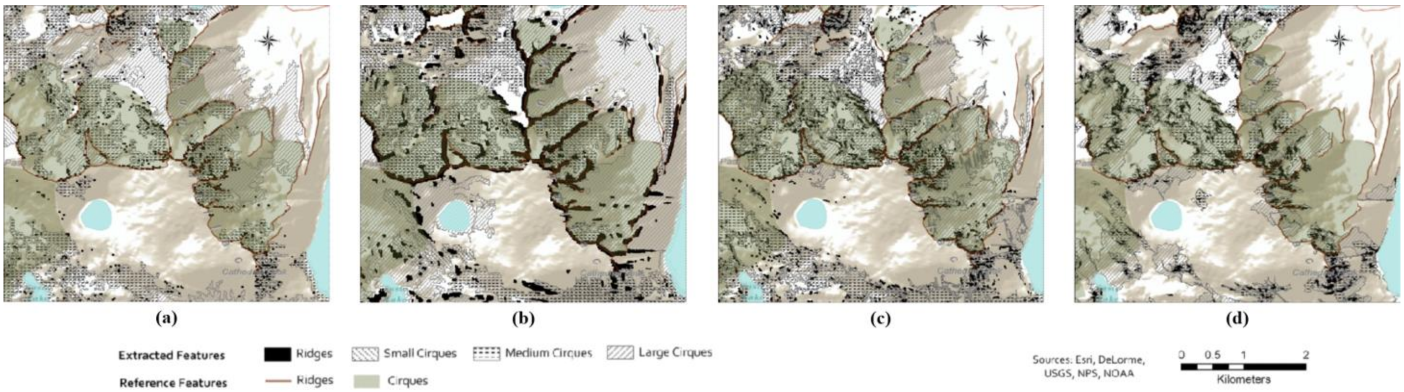

Figure 3. Ridges and cirques extracted from the 3DEP one arc-second resolution (Figure 3a), one-third arc-second resolution (Figure 3b), one-ninth arc-second resolution (Figure 3c), and one-half meter resolution (Figure 3d) DEMs using the GEOBIA workflow, in the Mt Tallac region of the Tahoe Basin.

Non-ridge objects were then segmented at consecutive SPs as specified by the Estimation of Scale Parameter tool [11] to create 12 test object levels. Objects in the test levels were classified as cirques where they had a negative mean curvature (concave), and bordered a ridge object. Adjacent cirque objects were then merged together and those smaller than 10 acres (~40,000 m^2) removed from the cirque class. Three size levels were chosen from each resolution to produce small, medium and large "cirque" datasets so that the choice of a single SP did not introduce unnecessary bias. The resulting ridge and cirque objects were compared visually and statistically to cirques manually circumscribed at a scale of ~1:10,000.

IV. Results and Discussion

A. *Visual assessment*

A smaller region around Mt Tallac, California, was used for the visual assessment, as it contains many cirques within a small area. Ridge extraction from the lowest resolution dataset (one arc-second, see Figure 3a) was fairly poor, and in many cases ridges are represented by disconnected objects, often just a few pixels or less in size. This is likely caused by too large of a pixel size of the DEM relative to the narrow width of ridges. Considering this shortcoming, extracted cirque features, particularly the large ones (run at high SP) resemble reference cirques remarkably well. The representation appears to fail greatest in classifying non-cirque objects as cirque objects (false positives), rather than in misclassifying cirque objects as non-cirque (false negatives).

Ridges derived from the one-third arc-second resolution DEM quite closely resemble the reference ridges (Figure 3b). Classified cirque objects match those of the reference cirques well, although in many cases they fail to capture the full extent of the cirque, increasing the number of false negatives. The classification, in general, displays fewer false positives than does the one arc-second classification.

Ridges classified from the one-ninth arc-second resolution DEM fail to match reference ridges well (Figure 3c). In particular, they are less linear and extensive. The classified cirques are more closely matched in extent to the reference cirques than those of the one-third arc-second DEM, particularly those created using the large SP. The classification generally exhibits more false positives, particularly in the southwest corner of the figure, than the one-third arc-second classification, but fewer false negatives than the one arc-second classification.

Ridges extracted from the half-meter DEM (Figure 3d) are similar to those of the one-ninth arc-second dataset. Cirque objects, however, fall short of the reference dataset, particularly along the northeast side of Mt Tallac where many large cirques exist in the reference dataset. False positive objects are seen in the southwestern part of the figure like the one-ninth arc-second extraction, but are not as extensive.

B. *Statistical assessment*

Five hundred random, stratified test points were generated automatically, and were assigned a value of 1 where they fell within a cirque and 0 where they did not (Figure 1). F^1 score was employed to compare the classification accuracy using different DEMs. This score is a quantitative measure based on the precision and recall of the classification relative to the reference dataset. Precision in our application measures the ratio of correctly classified cirque points over all points that have been classified as cirque points. Recall measures the ratio between correctly classified cirque points over all true cirque points. Mathematically, the F^1 score can be expressed as:

PeerJ Preprints | https://doi.org/10.7287/peerj.preprints.27072v1 | CC0 Open Access | rec: 30 Jul 2018, publ: 30 Jul 2018

$$F^1 = 2 \times \frac{1}{\frac{1}{recall} + \frac{1}{precision}} = 2 \times \frac{precision \times recall}{precision + recall}$$

Figure 4 demonstrates the F^1 scores for the retrival of cirque at different sizes. F^1 scores indicate that the one-third arc-second resolution DEM produces the best results in all three cirque sizes. The one-ninth arc-second DEM produced large objects with good results, and the one-arc second DEM produced large and medium objects with fair results. Interestingly, results were increasingly better from small to large objects for each resolution.

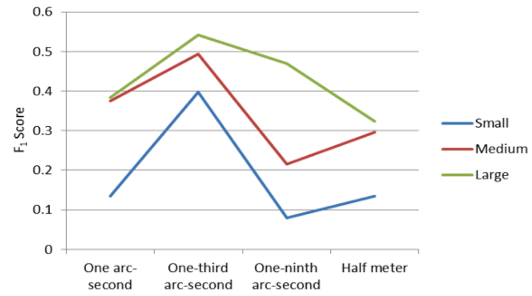

Figure 4. F^1 scores for three cirque sizes across four DEM resolutions.

The fact that the one-third arc-second dataset provided the best resolution to reproduce the reference dataset is likely due to (at least) two reasons. First, the pixel size itself is likely to be well-suited to the size of the natural features (cirques) themselves. Smaller pixels tend to produce more noise not related to the features of interest. Larger pixels, on the other hand, may smooth the DEM to the point of missing areas of extreme curvature. Secondly, the scale at which the reference features were digitized (1:10,000) falls between the working scales of the one-third (~1:24,000) and the one-ninth (~1:8,000), which might help explain why the one-ninth arc-second also performed well. It would be interesting to test the results relative to reference features derived at different scales, although such an approach would likely not be feasible in a real extraction case, as creating just one reference dataset is often too costly. In any case, the scale at which reference features are created should be taken into consideration when evaluating statistical comparisons between them and extracted features.

The variation in fit between extracted and reference features based on cirque size (scale parameter) can be as pronounced as that based on DEM resolutions. In fact, the average range of object size-based F^1 scores (0.27) was greater than that of the resolution-based F^1 scores (0.24). This suggests that the choice of object size (scale parameter) is as important as, and possibly more important than, the choice of DEM resolution. Certainly, it appears that both should be considered carefully before modelling terrain features using object-based image analysis.

V. Conclusion

Study results indicate that differing DEM resolutions can greatly impact the accuracy of extracted terrain features such as glacial cirques. DEM resolutions of working scales close to the reference feature scale should be chosen, as well as pixel sizes appropriate for mapping the proposed feature.

The chosen relative GEOBIA scale parameter was found to impact the accuracy of the extraction as much as does the DEM resolution. Therefore, resolution and scale choices in terrain feature extraction using GEOBIA techniques are doubly complicated, and must be contemplated thoroughly and wisely.

This work could be improved by including additional study areas, and expand to a range of terrain features. Additionally, it would be interesting to test extractions against reference features generated at various scales, particularly if those scales can more closely match the DEM working scales.

Acknowledgment

This research was funded by the National Geospatial Program as part of the U.S. Geological Survey.

References

[1] Drăguţ, L., and C. Eisank, 2009. "Object representations at multiple scales from digital elevation models." Geomorphology, 129, 183–189.

[2] Huang, X., K. Liu and L. Xiong, 2015. "The Influence of DEM Resolution on the Extraction of Terrain Texture." Geomorphometry, 123–125.

[3] Csillik, O., I. S. Evans, and L. Drăguţ, 2015. "Transformation (normalization) of slope gradient and surface curvatures, automated for statistical analyses from DEMs. Geomorphology, 232, 65–77.

[4] Minár, J, and I. S. Evans, 2008. "Elementary forms for land surface segmentation: The theoretical basis of terrain analysis and geomorphological mapping." Geomorphology, 95, 236–259.

[5] Tricart, J., and A. Cailleux, 1962. "Le modèle glaciaire et nival. Inf. Geogr. 28, 221 (1962).

[6] Evans, I. S., and N .J. Cox, 2015. "Size and shape of glacial cirques: comparative data in specific geomorphometry." Geomorphometry for Geosciences. 63, 79–82 (2015).

[7] Henry, C. D., 2009. "Uplift of the Sierra Nevada, California." 575–576.

[8] Basagic, H. J. I., 2008. "Quantifying twentieth century glacier change in the Sierra Nevada, California." Portland State University.

[9] Eisank, C., L. Drăguţ, J. Gotz, and T. Blaschke, 2015. "Developing a semantic model of glacial landforms for object-based terrain classification–the example of glacial cirques." GEOBIA, 1682-1777.

[10] Arundel, S. T., 2016. "Pairing semantics and object-based image analysis for national terrain mapping - a first-case scenario of cirques." GEOBIA 2016 : Solutions and Synergies (eds. Kerle, N., Gerke, M. & Lefevre, S.) (2016).

[11] Drăguţ, L., D. Tiede, and S. R. Levick, 2010. "ESP: a tool to estimate scale parameter for multiresolution image segmentation of remotely sensed data." Int. Journal of Geographical Information Science, 24, 859-871.

PeerJ Preprints | https://doi.org/10.7287/peerj.preprints.27072v1 | CC0 Open Access | rec: 30 Jul 2018, publ: 30 Jul 2018